CrossMark

Regeneration cathode material mixture from spent lithium iron phosphate batteries

Lihua Wang[1] · Jian Li[1,2] · Hongming Zhou[1,2] · Zuqiong Huang[1] · Shengdong Tao[1] · Bingkun Zhai[1] · Liangqin Liu[1] · Leshan Hu[1]

Abstract

Cathode materials mixture ($LiFePO_4$/C and acetylene black) is recycled and regenerated by using a green and simple process from spent lithium iron phosphate batteries (noted as S-LFPBs). Recovery cathode materials mixture (noted as Recovery-LFP) and Al foil were separated according to their density by direct pulverization without acid/alkali leaching for the first time. Subsequently, Recovery-LFP is further directly regenerated with solid state reaction and reused for lithium ion battery without adding acetylene black at the first time. Compared with recovery material, regeneration cathode materials mixture (noted as regeneration-LFP) displays excellent electrochemical performances, which delivers a discharge capacity of 129.43 mAh g^{-1} in the first and maintains 120.32 mAh g^{-1} with a high capacity retention rate of 92.96% after 1000 cycles at 0.5C through 18,650 battery testing. It is concluded that the regeneration material can be reused as cathode materials for lithium batteries.

1 Introduction

Rechargeable lithium-ion batteries (LIBs) have been commercialized for many years, due to their superior performance including high energy/power densities, long cycle life, memoryless effect and environmentally friendly property [1–4]. $LiFePO_4$/C as a type of cathode materials for Li-ion battery have been applied to electric vehicles (EVs) and hybrid electric vehicles (HEVs) [5–8]. However, the span of lithium iron phosphate batteries is about 3–5 years depending on the usage and the quality of the batteries. When using batteries for an extended period of time, the original materials structure and content change, resulting in rapid capacity fading. When the batteries are retired, which will cause the severe harm to the environment on account of irregular management or improper treatment. Therefore, a lot of spent LFP batteries will be produced and need to be recovered using green ways.

Up to now, conventional recycling methods for $LiCoO_2$, $LiMn_2O_4$ or mixtures are used to recover valuable metals, which can be reused for manufacturing new electrode materials [9, 10]. Nguyen et al. [11] researched separation and recycling cobalt, nickel, and lithium from LIBs. High purity (99.9%) cobalt sulfate along with Ni and Li is recovered by solvent extraction. Higuchi et al. [12] investigated selective recovery of lithium from manganese-type, cobalt-type, nickel-type, and ternary-type batteries, used by sodium persulfate ($Na_2S_2O_8$) and sodium carbonate (Na_2CO_3). Li yang, et al. [13] re-synthesized $LiNi_{1/3}Mn_{1/3}O_2$ by using a combination of dissolution, co-precipitation, calcination. Li et al. [14] recycled metal values from spent LIBs firstly by hydrometallurgy, followed by the preparation of $LiCoO_2$. Li et al. [15] re-synthesized $LiCoO_2$ from spent LIBs by leaching and a sol–gel method and calcined at high temperature.

Compared to the above-mentioned cathode materials, lithium iron phosphate batteries contain inexpensive metal except Li, which will contribute to decrease cost of the research of S-LFPBs. Bian et al. [16] synthesized $LiFePO_4$/C from S-LFPBs. Spent $LiFePO_4$/C cathode materials were leached by phosphoric acid (H_3PO_4) solution in order to obtain $FePO_4 \cdot 2H_2O$. Re-synthesized $LiFePO_4$/C was prepared to obtain $FePO_4 \cdot 2H_2O$ precursor, Li_2CO_3 and glucose. Li et al. [17] designed a "spent LFP batteries → NaOH solution used in separation of Al and cathode material mixture

✉ Hongming Zhou
 zhouhongming@csu.edu.cn

1 School of Materials Science and Engineering, Central South University, Changsha 410083, Hunan, China

2 Hunan Zhengyuan Institute for Energy Storage Materials and Devices, Changsha 410083, Hunan, China

→ recycling cathode material mixture (LFP/C and acetylene black) → regenerated LFP/C material" recycling process. Recycled cathode material mixture without acid leaching is directly regenerated with Li_2CO_3 and reused for LIBs.

In this work, a new recycling process is researched for cathode material mixture from S-LFPBs, without causing secondary pollution. Cathode material mixture ($LiFePO_4$/C, adhesive and acetylene black) and Al powder without acid or base are directly crushed by a crushing machine and sieved in one particular environment. Recycled cathode material mixture is regenerated with solid state reaction and reused for LIBs without adding acetylene black. Surface configuration, structural characterization and electrochemical performance from regeneration materials are investigated in detail. Recovery-LFP is obtained from S-LFPBs without heat treatment. Regeneration-LFP is acquired from Recovery-LFP under high temperature.

2 Experimental

2.1 Recycled cathode material mixture

S-LFPBs (voltage ≈ 1.5 V) used in this work were from market, which were discharged to 0.5 V. In the dry and sealed environment, use the angle grinder to dismantling batteries, then separate battery cells and shells. Battery cells were washed three times by DMC solution, and dried under 95 °C for 24 h. Then, separated cathode electrodes by hands, and smashed by pulverizer, recycled cathode material mixtures were obtained through removed aluminum powder by sifters. Recycled cathode material mixtures were further directly regenerated at 300 °C for 2 h and 750 °C for 7 h in high purity N_2 atmosphere (Fig. 1).

Fig. 1 Direct regeneration process flow diagram of cathode material mixture from spent $LiFePO_4$ batteries
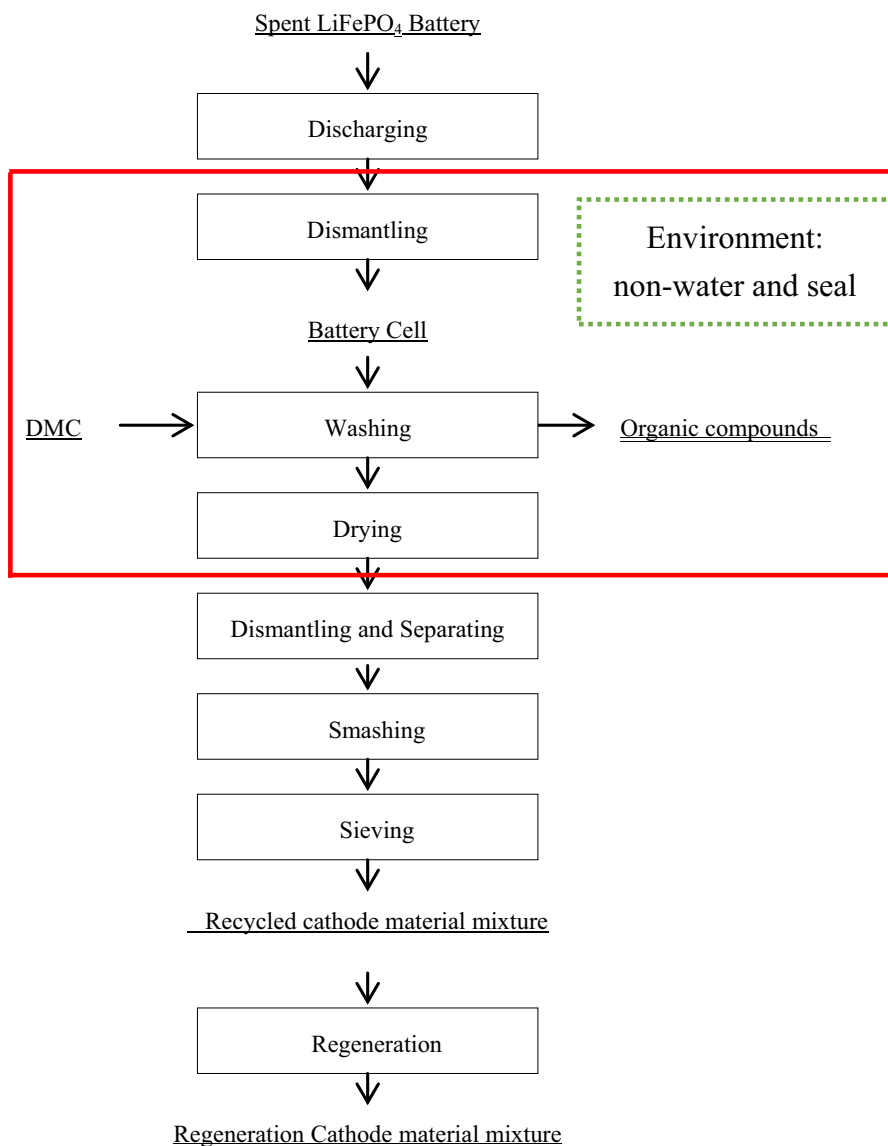
## 2.2 Compositional and structural characterization of cathode material mixture

The element composition and concentrations in the regeneration/recovery materials were determined utilizing ICP-OES (Blue, Spectro). Surface configuration and crystal structure of samples were characterized by scanning electron microscope (SEM, Tescan, MIRA 3 LMU), transmission electron microscopy (TEM, Tecnai G2 F20) and X-ray diffraction (XRD, Siemens D 500). Particle size distribution were measured using particle size analyzer (Bettersize, 9300s), presence of carbon is characterized by Raman spectra (LabRAM HR800).

2.3 Electrochemical measurements

The Recycled and regeneration cathode material mixtures electrodes were punched from Al foil current collector coated with slurry of powder, poly (vinyl difluoride) (PVDF) and conductive Super-P in N-methyl-2-pyrrolidinon (NMP) at a weight ratio of 80:10:10. Lithium foil served as counter and reference electrode. CR2032 were assembled in an argon-filled glove box (Mbraunlab Master130, Germany), using metallic lithium foils as counter electrodes and Celgard ® 2325 as separators. The electrolyte was 1M $LiPF_6$ dissolved in a mixture of dimethyl carbonate (DMC), diethyl carbonate (DEC) and ethylene carbonate (EC) (1:1:1 by weight). CR 2032 was tested on a multi-channel battery test system (NEWARE). Galvanostatic discharging/charging cycling was performed at several different current densities between cutoff potentials of 2.0–3.8 V. Cyclic voltammetry (CV) at a scan rate of 20 mV s^{-1} and electrochemical impedance spectroscopy (EIS) in the frequency range of 0.1 MHz–0.01 Hz were tested on the CH instrument 660D electrochemical workstation.

3 Results and discussion

Environmental issues should not be ignored in the using process of LIBs, due to the harmful substances (such as DMC, DEC, EMC (ethyl methyl carbonate), EC and $LiPF_6$) contained in electrolyte in LIBs. Especially, $LiPF_6$ reacts with trace water to produce LiF, 2HF and POF_3, as the reaction (1) [18, 19].

$$LiPF_6 + H_2O \rightarrow LiF + 2HF(gas) + POF_3(gas) \qquad (1)$$
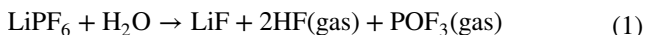
Dismantling process of S-LFPBs is conducted in one particular environment which is waterless and sealed, ensuring that electrolyte can not be decomposed and leaked into environment before recycled. The electrolyte in battery packs is recycled by washing with DMC. Recycled process doesn't produce harmful waste gas and waste water, and all whole process without acid/alkali leaching, so it can be considered as a completely recyclable process.

The element composition and concentrations of recovery/regeneration-LFP are given in Table 1 (analyzed by ICP-OES). Recovery/regeneration-LFP is composed of 4.29% Li along with 35.01% Fe, 20.93% P and 0.5% Al. Al performs as impurity in both materials. The mole ratio of Li:Fe:P is 0.98:1:1.08. What's more, some impurities such as carbon black, PVDF, graphite or other additives may exist in Recovery - LFP materials.

XRD is utilized to analyze the crystal structure as well as impurity of recovery materials and regeneration materials in Fig. 2, all the diffraction peaks of both samples match well with orthorhombic olivine $LiFePO_4$ structure (JCPDS: 83-2092). The impurities ($FePO_4$ and P_2O_5) of Recovery-LFP are caused by the decomposition of part of $LiFePO_4$ after numerous cycles [17]. $FePO_4$ is eliminated by the regeneration process, but P_2O_5 still exists on account of the excessive P (Table 1). The carbon peaks of Regeneration-LFP become weak, indicating that part of carbon could be coated in $LiFePO_4$ (Fig. 4c).

The presence of carbon in the samples is further characterized by Raman spectra. Figure 3 displays the Raman spectra of both samples in the 1100~1650 cm^{-1}. In two samples, the peaks at ~1300 and ~1600 cm^{-1} are ascribed to D-band and G-band, respectively. The D-band stands for the disorders or defects in the graphite structure, whereas G-band is attributed to the graphite carbon [20]. The value of the ID/IG (the intensity ratio of D band to G band) for Recovery-LFP and Regeneration-LFP is 1.04 and 0.86, respectively, which implies more graphitic-like carbon with higher electronic conductivity of Regeneration-LFP. Therefore, it has excellent the electrochemical performance, this is confirmed by the later 18,650 battery performance [21].

From Fig. 4a, serious agglomeration phenomenon and irregular particle size are observed in Recovery-LFP, due to residual PVDF binder and conductive additive. From Fig. 4b, the changes of morphology and reduction of agglomeration were observed in the Regeneration-LFP because of the decomposition of residual PVDF binder, which are consistent with particle size distribution curves of Recovery/Regeneration-LFP (Fig. 4d). From elemental mapping (Fig. 4), a small amount of C and Al elements are uniformly distributed in Regeneration-LFP. Figure 5 shows

Table 1 Chemical composition of recovery-LFP and regeneration-LFP

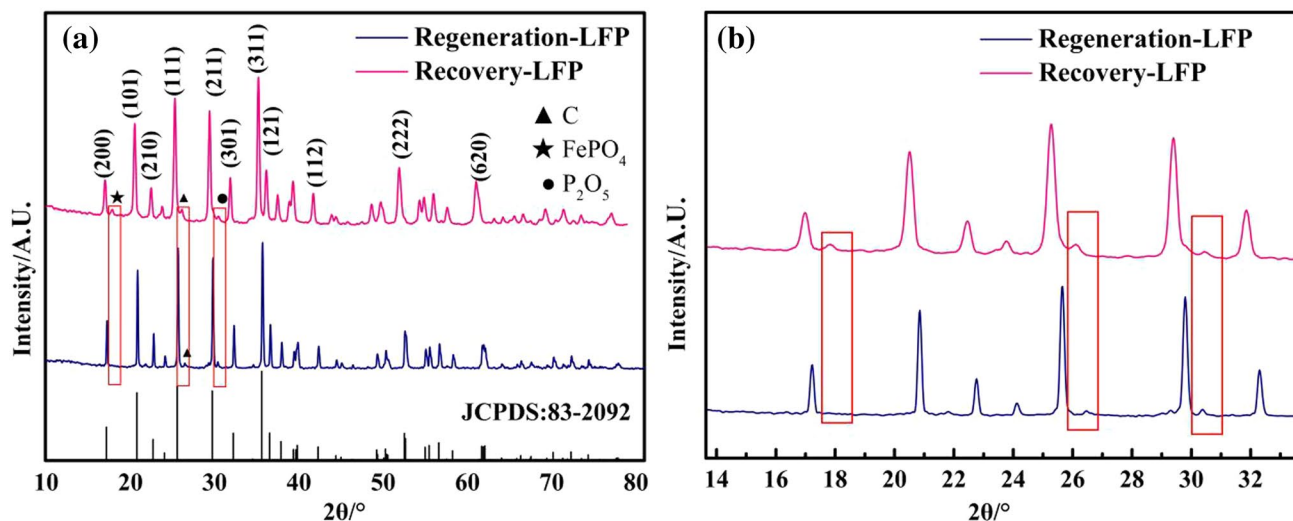| Element	Li	Fe	P	Al	M (Li:Fe:P)
Recovery/regeneration-LFP (wt%)	4.29	35.01	20.93	0.5	0.98:1:1.08

Fig. 2 XRD patterns **a** of recovery-LFP and regeneration-LFP. **b** Is a local enlargement of **a**
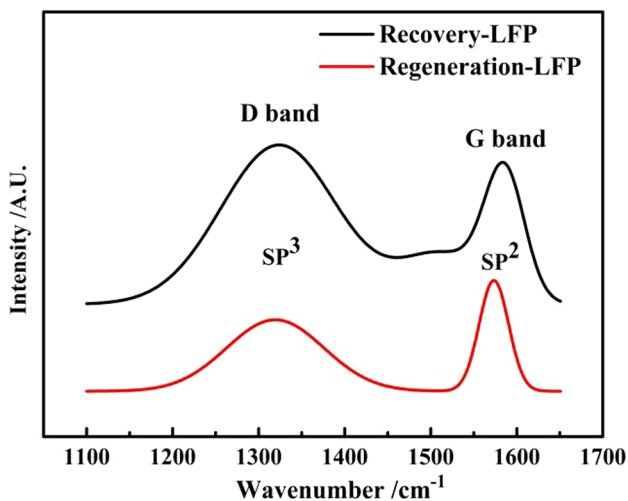

Fig. 3 Raman spectra of recovery-LFP and regeneration-LFP from spent $LiFePO_4$ batteries

the schematic illustration of the regeneration process for Recovery-LFP from the spent lithium ion phosphate batteries. PVDF can be turned into liquid wetting $LiFePO_4$/C in molten state, so $LiFePO_4$/C paticles are converged by the capillary force at calcination. PVDF is decomposed into C [as the reaction (2)] co-coated layers of intrinsic $LiFePO_4$/C or conductive particles, resulting in non-uniform thickness of coated layers outer surface of $LiFePO_4$ (Fig. 4c). They could grow into a bigger multiple particles between $LiFePO_4$/C and conductive additive. It is seen that more amorphous carbon covered around $LiFePO_4$/C at regeneration materials which enhanced conductive between particles (corresponding with Fig. 2).

$$[C_2H_2F_2]_n \xrightarrow{\text{thermolysis}} nHF(gas) + nC \qquad (2)$$
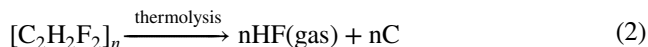
Figure 6a show the charge–discharge curves of Recovery/Regeneration-LFP. Contrast that with $LiFePO_4$/C in the market, the capacity at 0.2C is adopted. Recovery/Regeneration-LFP displays the maximum discharge specific capacity of 122.48 and 150.99 mAh g^{-1} in the 1st cycle at 0.2C, and coulomb efficiency (Percentage of discharge capacity and charge capacity) of 86.89 and 95.81%, respectively, and Regeneration-LFP has a smaller ΔV, because carbon without organism in the materials formed a consecutive carbon conductive film over the particles surface (as shown from TEM images in Figs. 4c and 5), which is improved the conductivity and contact between the active phase and the electrolyte [22]. The cycling performance of the two samples is shown in Fig. 6b, it can be seen that Regeneration-LFP exhibits superior cycling performance compared with its counterpart and delivers a discharge capacity of 147.29 mAh g^{-1} in the first and maintains 140.05 mAh g^{-1} with a high capacity retention rate of 95.08% after 100 cycles at C/3. However, The Recovery - LFP delivers a discharge capacity of 134.67 mAh g^{-1} in the first and only has 108.57 mAh g^{-1} with a capacity retention rate of 80.6% after the same cycles, suggesting that regeneration material has high reversible capacity and excellent cycling stability (in accord with Fig. 7).

Figure 6c shows the rate capabilities of both samples at various C-rates from 0.1 to 20C and 5 cycles are performed at a given rate. Compared with that of the Recovery-LFP, the discharge capacity of Regeneration-LFP is greatly enhanced at rates, which exhibited a better rate performance with a capacity of 99.96 mAh g^{-1} at a
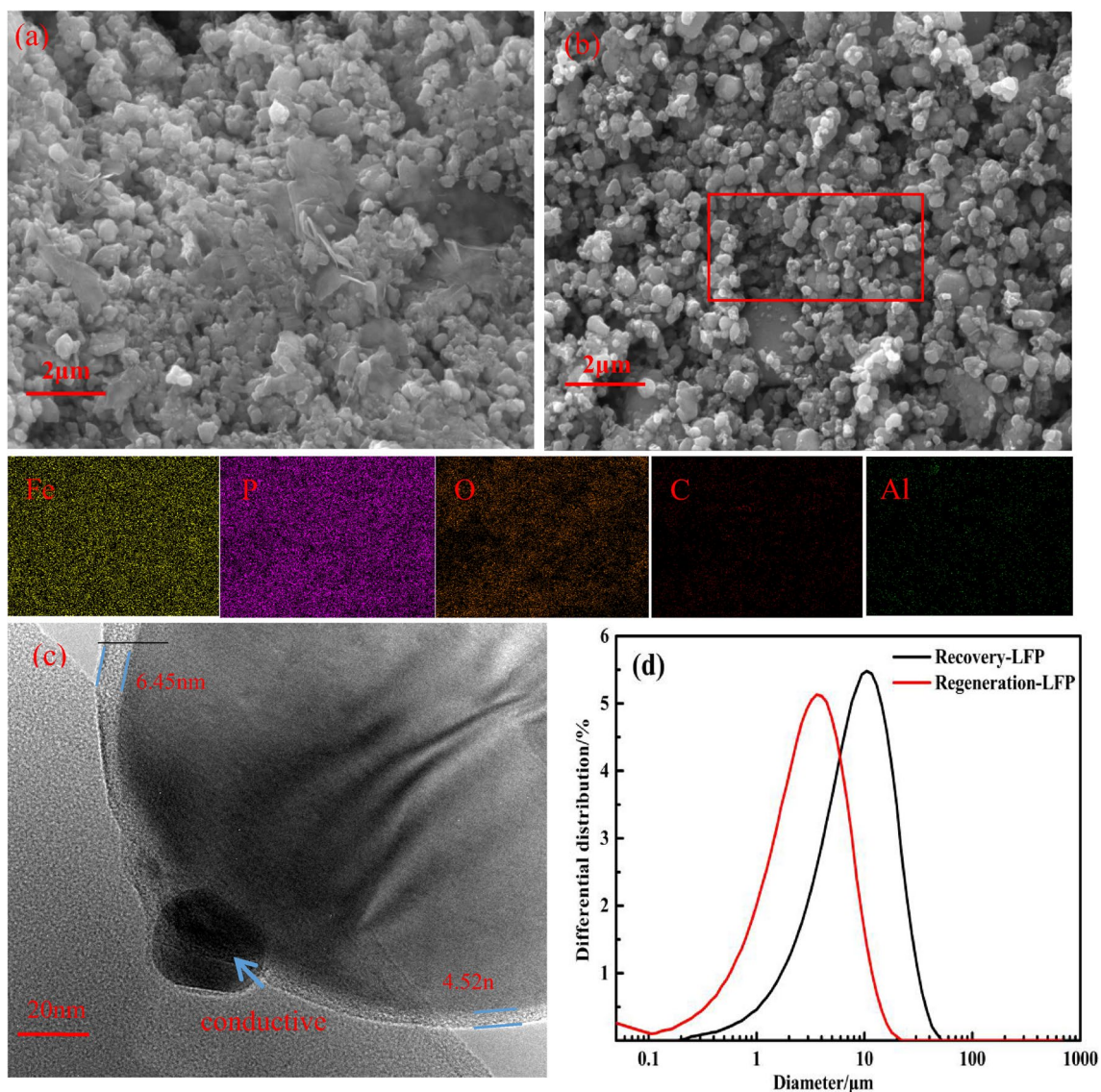
Fig. 4 SEM images of **a** Recovery-LFP, **b** Regeneration-LFP, elemental mapping of Fe, P, O, C, Al for Regeneration-LFP; TEM images of **c** Regeneration-LFP, Size distribution data **d** of both samples
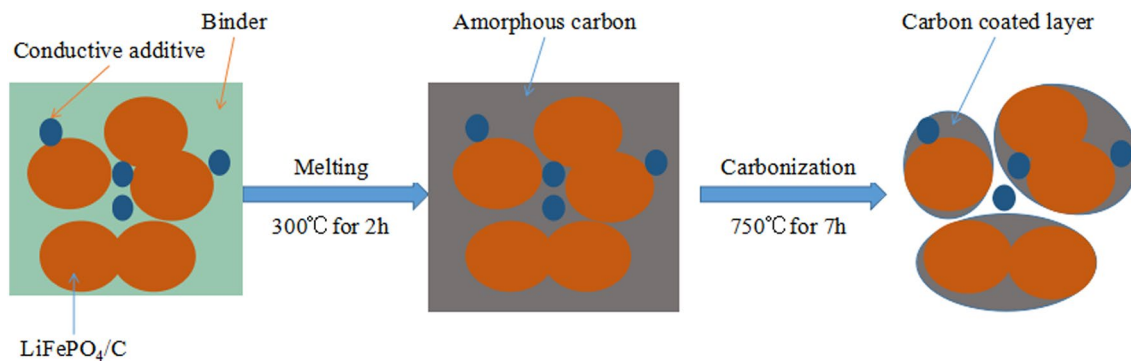

Fig. 5 Schematic illustration of the regeneration process of recovery-LFP from the spent lithium ion phosphate batteries
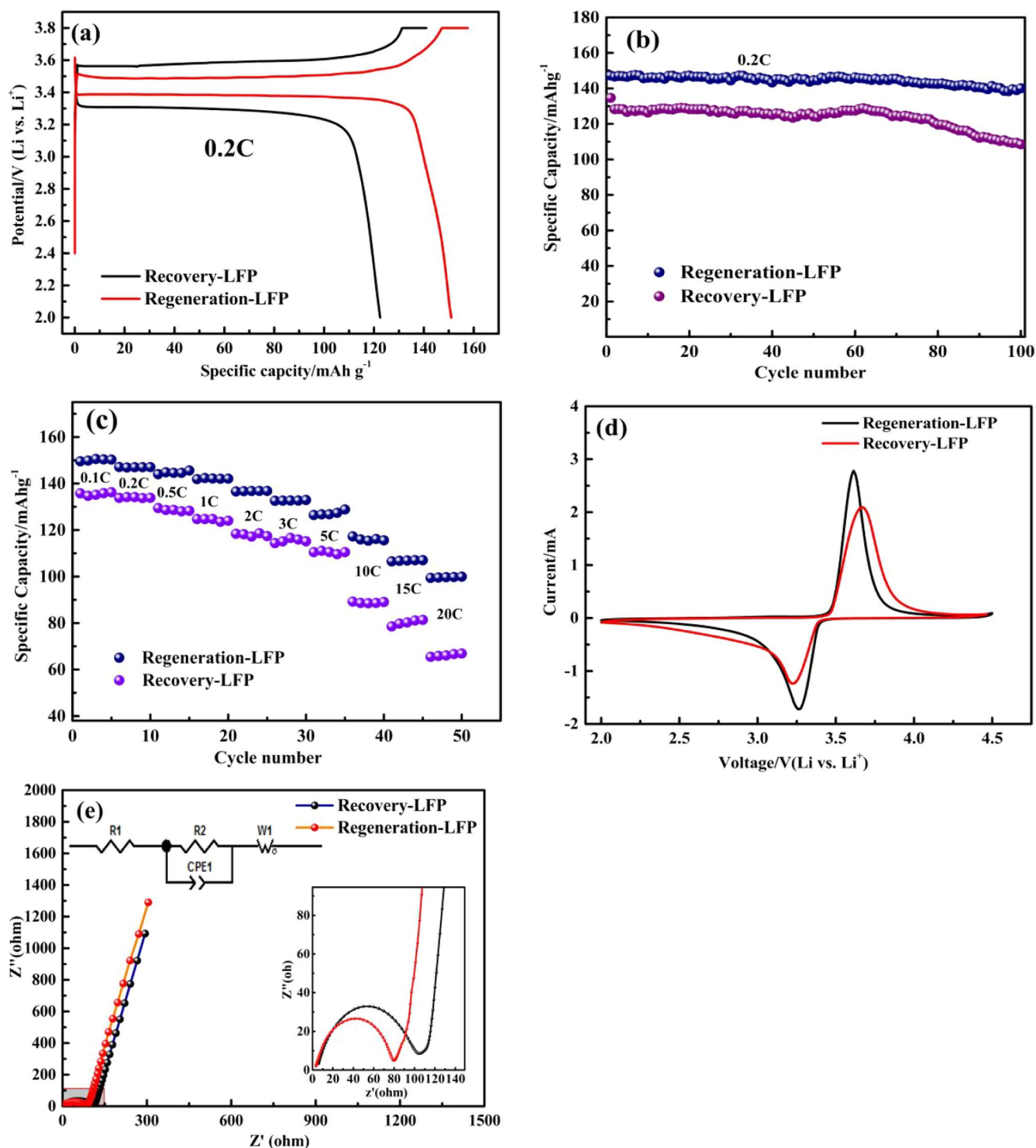
Fig. 6 **a** Charge–discharge curves, **b** cycling performance, **c** rate performance of Recovery/Regeneration-LFP versus Li/Li$^+$ in the voltage range of 2–3.8 V; **d** cyclic voltammetry curves of Recovery/Regeneration-LFP versus Li/Li$^+$ in the voltage range of 2.0–4.5 V at the scan rate of 0.5 mV s^{-1}; **e** the electrochemical impedance spectra (EIS) curves of Recovery/Regeneration-LFP versus Li/Li$^+$ in the frequency range from 1000 kHz to 10 mHz. The inset shows the equivalent circuit that is used to fit the experimental data

relatively high rate of 20C, whereas that of Recovery-LFP is 66.89 mAh g^{-1}, which is a highly desirable property for Regeneration-LFP from S-LFPBs.

Figure 6d shows the CV profiles of Recovery/Regeneration-LFP in the voltage range from 2.0 to 4.5 V at a scan rate of 0.5 mV s^{-1}. The one pair of redox peaks are well
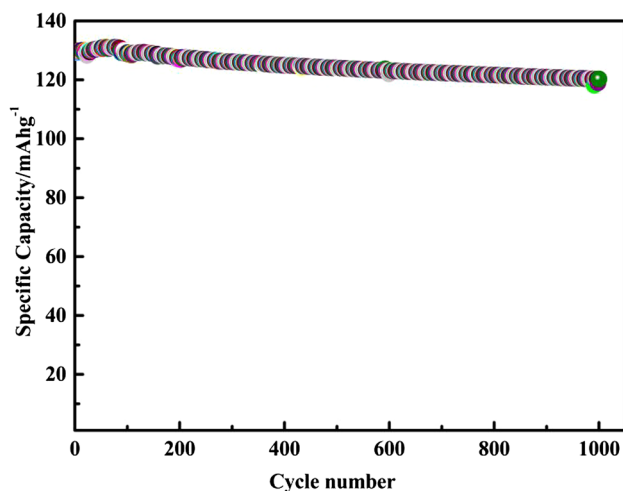
Fig. 7 Cycling performance of Regeneration-LFP at the rate of 0.5C in the voltage range of 2–3.8 V using 18,650 battery

consistent with the charge/discharge plateaus, further confirming the important lithium ion intercalation/deintercalation process of LiFePO$_4$/C in LIBs. Regeneration-LFP samples show a high peak current and a low potential difference (0.34 V), which is less than 0.44 V for Recovery-LFP. This result implies that the Regeneration-LFP sample exhibits a good reversibility with an extremely low polarization corresponding to the best cycling performance.

To further understand the reason for the improved electrochemical performance, the electrochemical impedance spectroscopy (EIS) measurements of Recovery/Regeneration-LFP electrodes in LIBs are performed. The EIS spectrum is measured by applying an AC voltage with a perturbation amplitude of 5 mV in the frequency range from 0.1 MHz to 0.01 Hz at open circuit potential. Figure 6e shows the Nyquist plots of Recovery/Regeneration-LFP electrodes. The depressed semicircles are attributed to the interfacial charge transfer reaction (Rct) in the cathode-electrolyte interface and the resistances of the Li$^+$ transport through the SEI film (Rsei), which mainly result from the electrode and electrolyte. The sloped lines in the low frequency region is attributed to the Warburg impedance (W) and associated with the solid state Li-ions diffusion into the electrode materials [23, 24]. The EIS data are analyzed by fitting to an equivalent circuit (Fig. 6e), it can be clearly observed that the charge transfer resistance (Rct) of Regeneration-LFP is significantly smaller than that of Recovery-LFP, as well as the SEI interface, which is attributed to PVDF in Regeneration-LFP decomposed to HF deteriorated LiFePO$_4$/C particles internal structure during regeneration procedure [17]. Meanwhile, it indicates that the Regeneration - LFP electrode has lower ion transfer resistance, which might be mainly attributed to the effective of the carbon coating and less content of impurities.

Cycling performance of Regeneration-LFP at the rate of 0.5C in the voltage range of 2–3.8 V using 18,650 battery is shown in Fig. 7, it can be seen that Regeneration-LFP delivers a discharge capacity of 129.43 mAh g^{-1} in the first and maintains 120.32 mAh g^{-1} with a high capacity retention rate of 92.96% after 1000 cycles. Therefore, Regeneration-LFP has very excellent cycling stability, it is concluded that the regeneration cathode material mixture can be reused as cathode materials for lithium batteries.

4 Conclusion

Recovery-LFP and Al foil were separated according to their density by direct pulverization without acid/alkali leaching. Through direct regeneration process, Regeneration-LFP from spent lithium iron phosphate batteries are reused in Lithium ion batteries. Regeneration-LFP display excellent electrochemical performances, which show the maximum discharge specific capacity and coulomb efficiency of 150.99 mAh g^{-1} and 95.81% at 0.2C rate and exhibite a better rate performance with a capacity of 99.96 mAh g^{-1} at a relatively high rate of 20C (Li vs. Li$^+$). Using 18,650 battery testing, it delivers a discharge capacity of 129.43 mAh g^{-1} in the first and maintains 120.32 mAh g^{-1}with a high capacity retention rate of 92.96% after 1000 cycles at 0.5C. It is concluded that the Regeneration-LFP can be reused as cathode materials for lithium ion batteries.

Compliance with ethical standards

Conflict of interest The authors declare there is no conflicts of interest regarding the publication of this paper.

References

1. X.F. Tu, Y.K. Zhou, X.H. Tian, Y.J. Song, C.J. Deng, H.X. Zhu, Electrochim. Acta **222**, 64–73 (2016)
2. J.M. Tarascon, M. Armand, Nature **414**, 359–367 (2001)
3. J.B. Goodenough, Y. Kim, Chem. Mater. **22**, 587–603 (2010)
4. K.E. Aifantis, S.A. Hackney, J.P. Dempsey, J. Power Sources **165**, 874–879 (2007)
5. B. Kang, G. Ceder, Nat. Lett. **458**, 190–193 (2009)
6. C. Delmas, M. Maccario, L. Croguennec, F.L. Cras, F. Weill, Nature **7**, 665–671 (2008)
7. L. Bao, L.L. Li, G. Xu, J.W. Wang, R.Y. Zhao, G. Shen, G.R. Han, S.X. Zhou, Electrochim. Acta **222**, 685–692 (2016)
8. X.H. Tian, Y.K. Zhou, G. Wu, P.C. Wang, J. Chen, Electrochim. Acta **229**, 316–324 (2017)
9. J. Ordoñez, E.J. Gago, A. Girard, Renew. Sust. Energy Rev. Renew. **60**, 195–205 (2016)

10. T. Zhang, Y.Q. He, F.F. Wang, L.H. Ge, X.N. Zhu, H. Li, Waste Manag. **34**, 1051–1058 (2014)
11. X.H. Zheng, W.F. Gao, X.H. Zhang, M.M. He, X. Lin, H.B. Cao, Y. Zhang, Z. Sun, Waste Manag. **60**, 680–688 (2017)
12. G.R. Nayaka, K.V. Pai, J. Manjanna, S.J. Keny, Waste Manag. **51**, 234–238 (2016)
13. L. Yang, G.X. Xi, J. Electron. Mater. **45**, 301–306 (2016)
14. V.C.B. Pegoretti, P.V.M. Dixini, P.C. Smecellato, S.R. .Biaggio, M.B.J.G. Freitas, Mater. Res. Bull. **86**, 5–9 (2017)
15. L. Li, R.J. Chen, X.X. Zhang, F. Wu, J. Ge, M. Xie, Chin. Sci. Bull. **57**, 4188–4194 (2012)
16. D.C. Bian, Y.G. Sun, S. Li, Y. Tian, Z.H. Yang, X.M. Fan, W.X. Zhang, Electrochim. Acta **190**, 134–140 (2016)
17. X.L. Li, J. Zhang, D.W. Song, J.S. Song, L.Q. Zhang, J. Power Sources **345**, 78–84 (2017)
18. X.G. Teng, F.Q. Li, P.H. Ma, Q.D. Ren, S.Y. Li, Thermochim. Acta **436**, 30–34 (2005)
19. K. Kanamura, H. Tamura, S. Shiraishi, Z.I. Takehare, Electrochim. Acta **40**, 913–921 (1995)
20. G.H. Qin, Q.Q. Wu, J. Zhao, Q.Q. Ma, C.Y. Wang, J. Power Sources **248**, 588–595 (2014)
21. Y.D. Cho, G.T.K. Fey, H.M. Kao, J. Power Sources **189**, 256–262 (2009)
22. G.H. Qin, Q.Q. Ma, C.Y. Wang, Electrochim. Acta **115**, 407–415 (2014)
23. L. Li, A.O. Raji, J.M. Tour, Adv. Mater. **43**, 6298–6302 (2013)
24. Y.Q. Zhang, M.M. Jia, H.Y. Gao, J.G. Yu, L.L. Wang, Y.S. Zou, F.M. Qin, Y.N. Zhao, Electrochim. Acta **184**, 32–39 (2015)